Langmuir

Article

pubs.acs.org/Langmuir

Inactivation and Adsorption of Human Carbonic Anhydrase II by Nanoparticles

Anna Assarsson,[†] Isabel Pastoriza-Santos,[‡] and Celia Cabaleiro-Lago*[,†]

[†]Department of Biochemistry and Structural Biology, Lund University, PO Box 124, SE 221 00 Lund, Sweden

[‡]Departamento de Química Física, Universidade de Vigo, 36310 Pontevedra, Spain

Supporting Information

ABSTRACT: The enzymatic activity of human carbonic anhydrase II (HCAII) was studied in the presence of nanoparticles of different nature and charge. Negatively charged nanoparticles inhibit HCAII whereas no effect is seen for positively charged particles. The kinetic effects were correlated with the strength of binding of the enzyme to the particle surface as measured by ITC and adsorption assays. Moreover, conformational changes upon adsorption were observed by circular dichroism. The main initial driving force for the adsorption of HCAII to nanoparticles is of electrostatic nature whereas the hydrophobic effect is not strong enough to drive the initial binding. This is corroborated by the fact that HCAII do not adsorb on positively charged hydrophobic polystyrene nanoparticles. Furthermore, the dehydration of the particle and protein surface seems to play an important role in the inactivation of HCAII by carboxyl-modified polystyrene nanoparticles. On the other hand, the inactivation by unmodified polystyrene nanoparticles is mainly driven by intramolecular interactions established between the protein and the nanoparticle surface upon conformational changes in the protein.

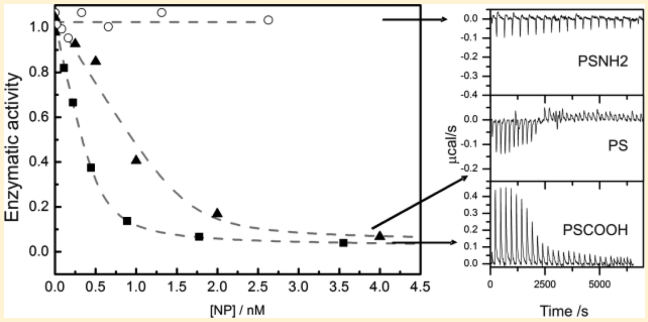

INTRODUCTION

Adsorption of protein on solid surfaces is a well-established phenomenon that has been reviewed extensively in the past.[1,2] Protein adsorption is of relevance to many applications of nanomaterials, for example biosensing, biocatalysis, or clinical diagnosis.[3−6] In many cases, passive adsorption is used as a method for protein immobilization. In this regard, quantitative knowledge about affinity constants, rates of adsorption, and coverage is important in order to design new efficient bionanomaterials. Moreover, depending on the area of application, undesired protein adsorption need to be avoided in order to preserve the functionality of the nanomaterial, as in the case inactivation by fouling in *in vivo* applications of biosensors.[7,8] Enzymes adsorption on surfaces can be exploited for the design of microreactors or biosensors, since high efficiency can be reached on nanoparticles and other nanomaterial through the high surface to volume ratio. However, interactions between nanoparticles and well-behaving enzymes could lead to unexpected negative effects due to changes in enzyme conformation that will lead to inactivation.[9,10] On the other hand, the inactivation of enzymes by nanomaterials can be exploited as a therapeutic method.[11−13]

Adsorption of a protein on a nanoparticle surface depends not only on external parameters such as ionic strength and temperature but also on the physicochemical properties of the protein and nanoparticle surface. The main driving forces for the adsorption are specific interactions between the protein and the surface, such as van der Waals forces or electrostatic interactions, dehydration of protein and nanoparticle interfaces, structural changes of the protein, and the lateral interaction between adsorbed proteins.[14] The adsorption depends on the proteins' properties such as the structural stability, composition, and size. The surface of the protein is not homogeneous. Despite the net charge of a protein, partial charges of opposite sign are distributed along the surface. The protein surface can also present hydrophobic and hydrophilic patches. Structural stable proteins can adsorb on its native conformation at the particle surface, "hard proteins". On the other hand, proteins with more conformational freedom, "soft proteins", adsorb and maximize the interaction by changing the protein conformation.

In order to gain more insight into the mechanism of protein adsorption on nanoparticles, the adsorption process and activity in the presence of polystyrene and gold nanoparticles were studied for a model protein human carbonic anhydrase II (HCAII).[15] HCAII is a well-characterized metalloenzyme that catalyzes the interconversion of carbon dioxide and water into bicarbonate and proton. Besides its biological activity, HCAII has esterase activity which allows easy monitoring of the enzymatic reaction by spectrophotometric methods.[16] HCAII has been shown to interact with hydrophilic negatively charged silica nanoparticles leading to loss of activity and conformational changes.[17] Moreover, carbonic anhydrases have been

Received: April 14, 2014
Revised: June 21, 2014
Published: July 7, 2014

   dx.doi.org/10.1021/la501413r | *Langmuir* 2014, 30, 9448−9456

used in bionanodevices for CO_2 sequestration.[18] In this work, the effects of hydrophobic particles (polystyrene and gold based particles) of different surface charge on the enzymatic activity of HCAII were studied as well as the binding affinity of the protein−particle complex and the conformational changes induced by the presence of the particles in order to get a full understanding of the driving forces behind the interactions between HCAII and the selected nanoparticles.

METHODS AND MATERIALS

Materials. Polystyrene nanoparticles with different surface modification (carboxyl-PSCOOH, amino-PSNH2, and unmodified PS) were purchased from Bang laboratories or Polysciencies. Particles were dialyzed against water to eliminate any additive or stabilizer. Poly(allylamine hydrochloride) (PAH, M_w = 15 000 g mol^{-1}), tetrachloroauric(III) acid, and trisodium citrate dihydrate were purchased from Sigma-Aldrich. Poly(sodium 4-styrenesulfonate) (PSS, M_w = 13 400 g mol^{-1}) was purchased from Polysciences. Buffers and salts and other chemicals were of the highest purity available.

Au Nanoparticles Synthesis and Surface Modification. 16 nm Au nanoparticles (NP) were prepared by standard citrate reduction.[19,20] The dimensions of the obtained gold nanospheres were 17 ± 3 nm, as determined by TEM analysis (Figure S1). Then these nanoparticles were coated with PAH followed by PAA as described by Schneider and Decher.[21]

30 nm AuNPs were obtained by growth of 16 nm AuNP seeds as described by Rodriguez-Fernandez[22] and coated with PSS, Au@PSS and then by PAH, Au@PSS@PAH, as described previously.[23] The dimensions of the obtained gold nanospheres were 30 ± 2 nm, as determined by TEM analysis (Figure S1).

Human Carbonic Anhydrase II. The protein ("pseudo wildtype" with C206S mutation) was expressed from the pCApwt plasmid (a kind gift from Professor Bengt-Harald Jonsson, Linköping University) in *E. coli* Bl21 De3 PlysS Star. The cells were harvested by centrifugation at 6000*g* for 5 min, and the pellet was frozen. The cell pellet was resuspended in 50 mM Tris/HCl, pH 7.4, sonicated, and centrifuged 10 min at 15 000 rpm twice. The supernatant was pumped onto a DEAE cellulose anion exchange column. Fractions with HCAII were dialyzed against water and freeze-dried. Freeze-dried protein was dissolved in buffer (50 mM Tris, 200 mM Na_2SO_4, pH 8) and loaded in an affinity column. The protein was eluted with 50 mM Tris/HCl, 0.4 M NaN_3, pH 7.0 buffer. Fractions with protein were pooled and dialyzed against water and freeze dried for further use.

Particle Characterization. Optical characterization was carried out by UV−vis−NIR spectroscopy with a Hewlett-Packard HP 8453 spectrophotometer. A JEOL JEM 1010 transmission electron microscope (TEM) operating at an acceleration voltage of 100 kV was used for particle size analysis and low-magnification imaging,

The hydrodynamic diameter and the ζ-potential of the nanoparticles were studied using a Malvern Zetasizer Nano S operating with a 632.8 nm laser and at a 173° scattering angle at 25 °C. Particles were dispersed either in water or in 5 mM Hepes/NaOH buffer pH 7.4. 5−10 measurements of each sample were taken using a clear disposable cuvette or a folded capillary cell (Malvern).

The hydrodynamic diameter of nanoparticles incubated with HCAII was studied using a Malvern Zetasizer Nano S or a DynaPro Plate reader II from Wyatt Technology operating with a 158° scattering angle at 25 °C. Samples were prepared in 10 mM Hepes/NaOH buffer pH 7.4 for different HCAII/nanoparticle ratios. 5−10 measurements of each sample were taken using a clear disposable cuvette or a 96-well black plate (Costar).

The intensity-averaged particle diameter and the polydispersity index values (an estimate of the distribution width) were calculated from cumulant-type analysis. Each value was averaged from 5−10 independent measurements and after at least 5 min of equilibration time.

Kinetic Measurements. The hydrolysis of *p*-nitrophenyl acetate (NPA) catalyzed by HCAII was monitored spectrophotometrically at 348 nm using a Hewlett-Packard 8453 UV−vis spectrophotometer fitted to a thermostatic unit. The substrate NPA was dissolved in acetronitrile to avoid hydrolysis prior to the initiation of the experiments. HCAII and nanoparticles were incubated in 5−10 mM Hepes/NAOH buffer at pH 7.4 for at least 10 min before the addition of the substrate. All experiments were performed at 25.0 ± 0.1 °C. The amount of acetonitrile in the sample was always less than 2% in volume. The reactions were followed up to 5 min, and the initial rate for each experimental condition was calculated from the initial linear range of the progression curve (when less than 2% of the product is produced). The initial rate of auto hydrolysis of NPA in water was subtracted from the initial rates of the enzymatically catalyzed reactions. Experiments were reproducible within 5% error.

If we assume that the particles have n identical and independent protein binding sites (NPs) and that the complex NPs-protein can have a residual enzymatic activity, a modified version of the Morrison equation[24] for the fractional activity (V_i/V_0) with the total concentration of the different reactants can be written (eq 1). V_i, V_0, and V_{NP} are the initial rates of the reaction in presence and absence of inhibitor and at the nanoparticle surface, respectively, and [E] and [E_t] the concentration of free and total enzyme.

$$\frac{V_i}{V_0} = \frac{[E]}{[E_t]} + \frac{V_{NP}}{V_0}\left(1 - \frac{[E]}{[E_t]}\right) \quad (1)$$

where

$$[E] = -\frac{1}{2}[(K_{iapp} - [E_t] + [NPs_t]) - \sqrt{(K_{iapp} + [E_t] - [NPs_t])^2 + 4[NPs_t]K_{iapp}}] \quad (2)$$

The concentration of binding sites at the particle surface [NPs_t] relates to the total nanoparticle concentration [NP_t] as follows:

$$[NPs_t] = n[NP_t] \quad (3)$$

By fitting this equation (OriginPro and/or Matlab) to the experimental data, the values for the stoichiometry of the complex, n, and the apparent inhibitor constant for each binding site, K_{iapp}, can be obtained.

Isothermal Titration Calorimetry (ITC). ITC experiments were performed using a VP-ITC instrument from Microcal (Northhampton, MA). HCAII was titrated from a 30−62 μM stock into the nanoparticle solution (9−15 nM) in 5 mM Hepes/NaOH buffer, pH = 7.4 at 25 °C. The first protein injection was 1 μL followed by a series of 10 μL injections. The content of the cell were continuously stirred at 480 rpm. Control titrations for the heat of dilution of the protein were performed by titrating HCAII into buffer at the same concentrations. The integrated heats for each experiment were calculated from the raw data and corrected for the integrated heat of dilutions in buffer. Different combinations of HCAII and nanoparticles concentrations and injection volumes were tested in separate experiments.

Data were analyzed using the Origin software (Microcal) assuming the single set of identical sites model (Supporting Information). By an iterative fitting procedure, the equilibrium dissociation constant K_d, n, and ΔH can be calculated.

Adsorption Assay. HCAII was incubated with nanoparticles at different concentrations (duplicates) in 5 mM Hepes/NaOH buffer, pH = 7.4, in a 96-well black plate (Costar). Control samples with only enzyme, only particles, and buffer alone were also prepared. Samples were transferred to an Acroprep Advanced filter plate (100 kDa molecular cutoff) and centrifuged 6 min at 1550*g*. The filtrated samples were collected in a 96-well black plate (Costar), and the absorption at 280 nm for each sample was obtained using a Hewlett-Packard 8453 UV−vis spectrophotometer. The fraction of free HCAII was obtained from the ratio between the absorption values for each sample and the sample without nanoparticles at each protein concentration to compensate for the unspecific binding to the membrane. The dissociation constant, K_d, and stoichiometry of the complex, n, was obtained by fitting the following equation to the

dx.doi.org/10.1021/la501413r | Langmuir 2014, 30, 9448−9456

experimental data (based on the Langmuir isotherm equation and the considerations explained previously in the Kinetic Measurements section)

$$\frac{[E_{bound}]}{[E_T]} = \frac{[NPs]}{[NPs] + K_d} \quad (4)$$

where

$$[NPs] = -\frac{1}{2}[(K_d + [E_t] - n[NP_t]) - \sqrt{(K_d + [E_t] - n[NP_t])^2 + 4n[NP_t]K_d}] \quad (5)$$

Circular Dichroism Spectroscopy. Far-UV CD spectra were recorded in a JASCO J-815 spectrometer in a 1 mm quartz cuvette at 25 °C using a scan rate of 20 nm/min. Spectra of 10 μM HCAII with additions of polystyrene nanoparticles up to 0.23 mg/mL in 5 mM Tris/H_2SO_4 buffer, pH 7.4, were measured in four accumulations. No difference was seen between the individual spectra. Data were collected at 1 nm intervals with a response time of 8 s and a band-pass of 1 nm. The change in buffer choice was required by the strong signal of the Hepes/NaOH buffer in the far-UV region. Kinetics experiments in Tris/HCl buffer show no significant variation in HCAII activity compared to the experiments performed in Hepes/NaOH (data not shown).

RESULTS

Characterization of Nanoparticles. The stability, size, and charge of the selected nanoparticles were investigated to ensure that the colloidal dispersion is stable and homogeneous under the experimental conditions chosen. The selected nanoparticles have hydrodynamic diameters between 30 and 60 nm (Table 1). The stability of the gold nanoparticles is easily monitored by UV−vis absorption spectroscopy, since they present a localized surface plasmon resonance band in the visible region which is very sensitive to the size and aggregation state of the nanoparticles.[25] Thus, while no time evolution of the localized surface plasmon resonance band was observed for Au@PSS and Au@PAH@PAA nanoparticles dispersed in buffer, the optical properties of Au@PSS@PAH colloids after dispersing in buffer slowly shifted toward longer wavelengths, which indicates aggregation. The stability of the polystyrene nanoparticles was investigated using DLS. All polystyrene nanoparticles were stable in the selected buffer for more than 24 h.

Table 1. Hydrodynamic Diameter, Polydispersity Index (PDI), and ζ-Potential for the Different Nanoparticles in Hepes/NaOH Buffer pH 7.4

nanoparticle	diameter (nm)	PDI	ζ-potential (mV)
Au@PSS	48 ± 10	0.14	−37 ± 2
Au@PSS@PAH	52 ± 2	0.12	53 ± 4
Au@PAH@PAA	31 ± 3	0.10	−28 ± 2
PSCOOH	43 ± 2	0.05	−44 ± 2
PS	46 ± 1	0.04	−41 ± 2
PSNH2	59 ± 2	0.07	42 ± 2

The ζ-potential of the nanoparticles was also measured. This is especially important for the gold nanoparticles since the ζ-potential value is a sign of a sufficient coating by polyelectrolyte. The particles show ζ-potential values around 30 mV or higher, either negative for PSCOOH, PS, Au@PSS, and Au@PAH@PAA or positive for PSNH2 and Au@PSS@PAH. The high negative potential of the unmodified polystyrene nanoparticles (PS) arises from residual groups from the polymerization reaction.

Stability of Nanoparticles in the Presence of Protein. The addition of protein can affect the characteristics and stability of the colloidal dispersion and thus compromise the kinetic and adsorption data. The adsorption on the particle surface could lead to an observable increase in the mean size of the nanoparticle or to aggregation due to screening of the electrostatic forces that keep the colloidal dispersion stable.

The size of the nanoparticles in the presence of HCAII was analyzed at the same experimental conditions as the kinetic experiments in order to ensure that the nanoparticles are stable in dispersion during the activity measurements. HCAII was titrated with increasing concentrations of polystyrene nanoparticles. The difference in size between the nanoparticles in buffer and in protein solutions was in all cases lower than 8 ± 3 nm for particle concentrations above 0.1 nM (Figure S2). A strong deviation from the average value was observed at low particle concentration caused by the low scattering signal in diluted colloidal dispersions.

The stability of the gold nanoparticles in the presence of HCAII was measured *in situ* using the plasmon band of the gold particles. All gold nanoparticles were stable within the time limits of the kinetic experiment; however, the positive charged gold nanoparticles start to slightly aggregate after 1 h incubation with HCAII.

However, the stability of the colloidal dispersion at high particle concentration (20 times higher) differs between the different particles. Figure 1 shows the variation of the mean peak position for the different nanoparticles when titrated with increasing concentrations of HCAII. The mean size as well as the width of the size distribution of PSNH2 does not show any variation with the addition of the protein which indicates no strong protein adsorption (Figure S3). On the other hand, the size distribution for PSCOOH and PS changes as more HCAII is titrated into solution (Figure 1 and Figure S3). The PSCOOH diameter increases smoothly from 43 ± 2 nm toward a plateau at 54 ± 1 nm. The plateau value can be interpreted as the mean hydrodynamic diameter of the PSCOOH−HCAII complex. PS diameter, which does not change for the first titrations, increases sharply when the concentration of protein further increases. The addition of protein increases the mean diameter and broadens significantly the size distribution (Figure

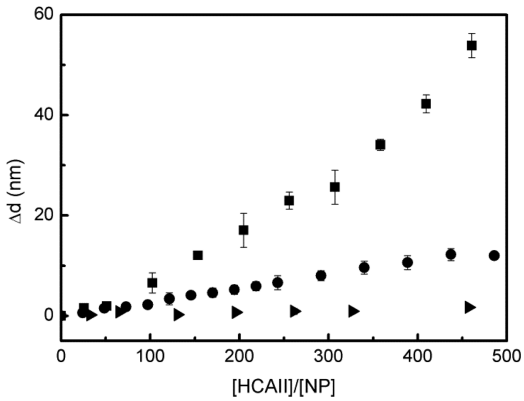

Figure 1. Variation of the hydrodynamic diameter of different polystyrene particles measured by DLS upon titration with HCAII in 5 mM Hepes/NaOH buffer at 25 °C: (●) PSCOOH, (■) PS, (▶) PSNH2. Errors bars show the standard deviation.

dx.doi.org/10.1021/la501413r | *Langmuir* 2014, 30, 9448−9456

S3), leading even to a bimodal size distribution. Furthermore, the nanoparticle−protein dispersion precipitates out of solution after few hours. These evidence support the idea that the presence, the adsorption of HCAII, or both destabilize the particle dispersion. Similar aggregation was observed for Au@PSS nanoparticles (data not shown).

Enzymatic Activity in the Presence of Nanoparticles. The effect of nanoparticles of different chemical composition and surface characteristic on the enzymatic activity of HCAII was studied by monitoring the esterase activity of the enzyme. The initial rate of the enzymatic hydrolysis of NPA was obtained for increasing concentrations of nanoparticles. The results show that the effect of the nanoparticles depends on the chemical nature of the nanoparticles surface (Figure 2). While

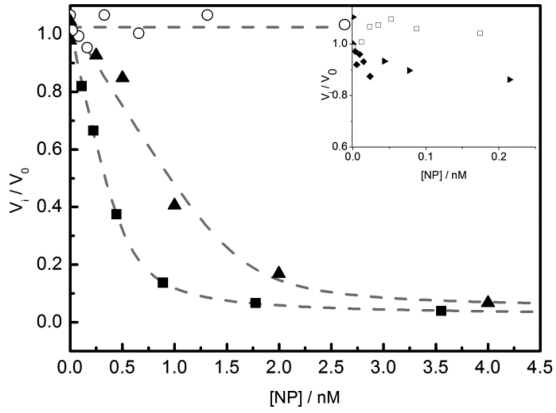

Figure 2. Fractional enzymatic activity (V_i/V_0) for the catalyzed hydrolysis of NPA by HCAII in the presence of nanoparticles: (■) PS-COOH, (▲) PS, (♦) Au@PSS, (▶) Au@PAH@PAA, (○) PS-NH2, (□) Au@PSS@PAH. [HCAII] = 0.36 μM; [NPA] = 1.7 mM in 10 mM Hepes/NaOH buffer pH 7.4. The initial rate of the autohydrolysis of NPA was subtracted from the total initial rate value. Dashed lines indicate best fitting of eq 1 to the experimental data.

the positively charged nanoparticles show no significant effect on the initial rate of the enzymatic reaction even when a wide range of nanoparticles concentration is explored, negatively charged nanoparticles inhibit the enzymatic reaction. The strongest effect is seen for the carboxyl-modified nanoparticles leading to a complete inhibition of the enzyme. The half-maximal inhibitory concentration, IC_{50}, is in the nanomolar region for PSCOOH and PS (0.3 and 0.6 nM, respectively). Nanoparticles show very low IC_{50} values since many enzymes can interact and being inhibited by a single nanoparticle due to the big surface area per volume of nanomaterials. The stoichiometry of the complex and the apparent dissociation constant obtained using the model presented in materials and methods are presented in Table 2.

Adsorption of Protein on the Particle Surface. The observed kinetic effects can be explained by adsorption of HCAII on the particle surface. The binding process of HCAII to the polystyrene nanoparticles (since they show the maximum inhibitory effect) was studied using ITC and an adsorption assay based on the depletion of protein from solution after being in contact with the nanoparticles. PSNH2 was used as a negative control according to the activity data. Unfortunately, the setup of these experiments is not suitable for the study of the binding process between gold nanoparticles and HCAII due to the low concentration of the nanoparticle stock solutions.

The ITC measurements show clearly a binding process between HCAII and PS and PSCOOH. On the other hand, no significant signal was obtained for PSNH2 even when the concentration of nanoparticles and protein where increased to the maximum level possible for the experimental conditions (Figure 3).

Despite the fact that both negatively charged polystyrene nanoparticles interact with HCAII, according to the ITC data the nature of the interaction is different. The binding between HCAII and PSCOOH is an endothermic process while the process between HCAII and PS is exothermic (Figure 3). The stoichiometry of the complex and the dissociation constant for a single site are summarized in Table 2 together with the thermodynamic parameters. However, care must be taken when drawing conclusions from the titration data for PS nanoparticle. The titration of PS nanoparticles with HCAII when nanoparticle concentration is high leads to particle aggregation (Figure 1). Therefore, the observed heat peaks may originate from aggregation processes as well as binding events. Thus, conclusions based on the obtained parameters can be compromised. Nevertheless, at the first injections aggregation was not observed in the DLS titration experiment (Figure 1). Consequently, even though the binding constant can be overestimated and stoichiometry underestimated, the ITC data show that HCAII interacts and adsorbs on PS and that the process is exothermic.

In order to confirm the binding process in the presence of nanoparticles, equilibrium filtration experiments were performed. As expected, the concentration of free protein in solution decreases as the concentration of PS and PSCOOH increases, indicating adsorption of HCAII on the particle surfaces (Figure 4). The values for the dissociation constant and stoichiometry of the protein−nanoparticle complex (Table 2) can be obtained by fitting a n independent and equal sites

Table 2. Stoichiometry, Coverage, Apparent Inhibitor Constant, Dissociation Constant, and Thermodynamic Parameters for the HCAII−Polystyrene Nanoparticle Interaction

	activity assay		ITC		adsorption assay	
	PSCOOH	PS	PSCOOH	PS	PCOOH	PS
stoichiometry (n)	646 ± 78	247 ± 100	409 ± 26	126 ± 14	553	503
coverage (%)[a]	111	32	70	16	95	64
K_{iapp} (10^{-9} M)	28 ± 11	18 ± 28				
K_d (10^{-9} M)			250 ± 180	17 ± 12	250	100
ΔH (10^4 kcal/mol)			3.6 ± 0.9	-3.8 ± 0.2		
ΔS (kcal/(mol K))			152 ± 30	−84 ± 1		

[a]Assuming a surface binding area for HCAII of 10 nm^2.

dx.doi.org/10.1021/la501413r | Langmuir 2014, 30, 9448−9456

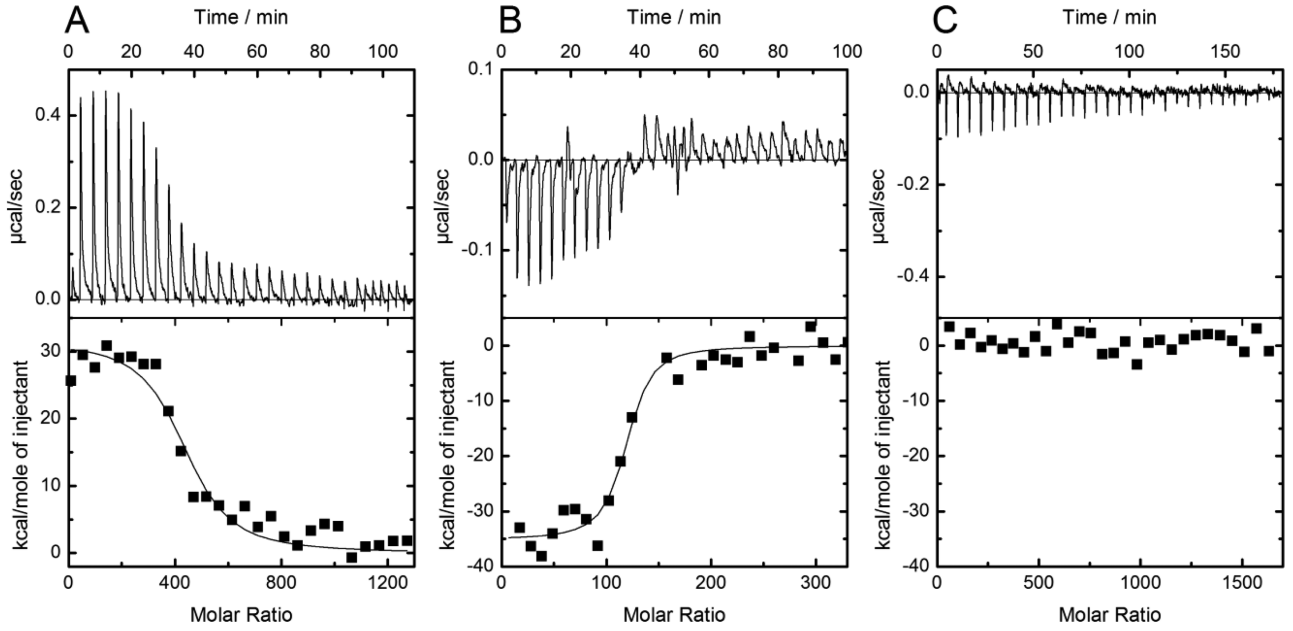

Figure 3. ITC data for the titrations of HCAII into solutions of different polystyrene nanoparticles in 5 mM Hepes/NaOH, pH 7.4 at 25 °C. (A) PS-COOH, [PS-COOH] = 9.8 nM, [HCAII] = 62 μM. (B) PS [PS] = 15 nM, [HCAII] = 30 μM. (C) PS-NH2, [PS-NH2] = 8.6 nM, [HCAII] = 62 μM. The upper panels show the raw data and the lower panels the integrated heats for each injection (■) and the best fit for a *n* independent and equal sites binding model (line).

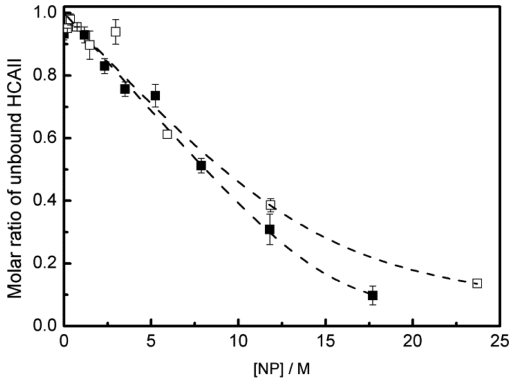

Figure 4. Variation of the molar ratio of unbound HCAII with the concentration of added negative polystyrene nanoparticles: (■) PSCOOH, (□) PS. [HCA] = 8μM, 5 mM Hepes/NaOH buffer pH 7.4 at room temperature. Dashed lines show the best fit of *n* independent and equal sites binding model to the experimental data.

binding model to the data under the assumptions described in the Materials and Methods section (eq 4).

An unexpected result was observed in the case of PSNH2 (Figure S4). The amount of protein in the filtrate increases with the addition of PSNH2, probably as an artifact of the experimental setup. The membrane used has some unspecific binding of the protein that prevents the 100% recovery of the protein. We suggest that the increase of protein in the filtrate is due to the release of unspecifically bound protein due to the competition between protein and PSNH2 for the binding sites of the filtration membrane. Despite the technical difficulties, we can conclude that PSNH2 nanoparticles do not form stable complexes with HCAII.

Conformational Changes. Far-UV CD was used to analyze the effect of the addition of nanoparticles on the secondary structure caused by the interaction of HCAII with the nanoparticle surface (Figure 5). HCAII shows a minimum at 210 nm in accordance with previously reported CD spectra.[26] On the other hand, the studied nanoparticles do not show any significant signal in the concentration range studied (Figure S5). The addition of negatively charged nanoparticles reduces the signal which indicates a modification of the secondary structure of HCAII. The variations on the signal may also reflect on changes in the tertiary structure since aromatic residues also contributes to the far-UV spectrum of HCAII.[26] The effect is stronger in the case of the PS nanoparticles. Small changes are observed for PSNH2 nanoparticles but no clear trend with the nanoparticle concentration is observed. The data suggest that HCAII interacts with PS and PSCOOH and the interaction leads to conformational changes of the protein. On the other hand, no or weak interactions occurs between HCAII and PSNH2.

■ DISCUSSION

Bionanomaterials, based on the modification of nanoparticle surfaces by relevant biomolecules, have been proposed and used for diverse applications such as medical diagnosis,[4] catalysis,[27] and therapeutics.[28] The adsorption at the particle surface can modify the properties of the adsorbed protein and in particular change the activity of adsorbed enzymes.

Adsorption and Inactivation. The enzymatic activity of HCAII is strongly affected by negatively charged nanoparticles while positively charged ones have no effect (Figure 2). In the case of negatively charged gold nanoparticles, full inactivation was not achieved due to limitations in particle concentration. The strongest effect is observed for the negatively charged polystyrene particles. At the highest PSCOOH and PS concentration used, the enzyme is completely inhibited after relatively short incubation times (up to 30 min). Previous reports show that HCAII is still active after short incubation times with silica nanoparticles and after 5 months incubation still retains 5% activity.[29] Hence, it can be concluded that the inactivation is much faster in the case of the negatively charged

dx.doi.org/10.1021/la501413r | *Langmuir* 2014, 30, 9448−9456

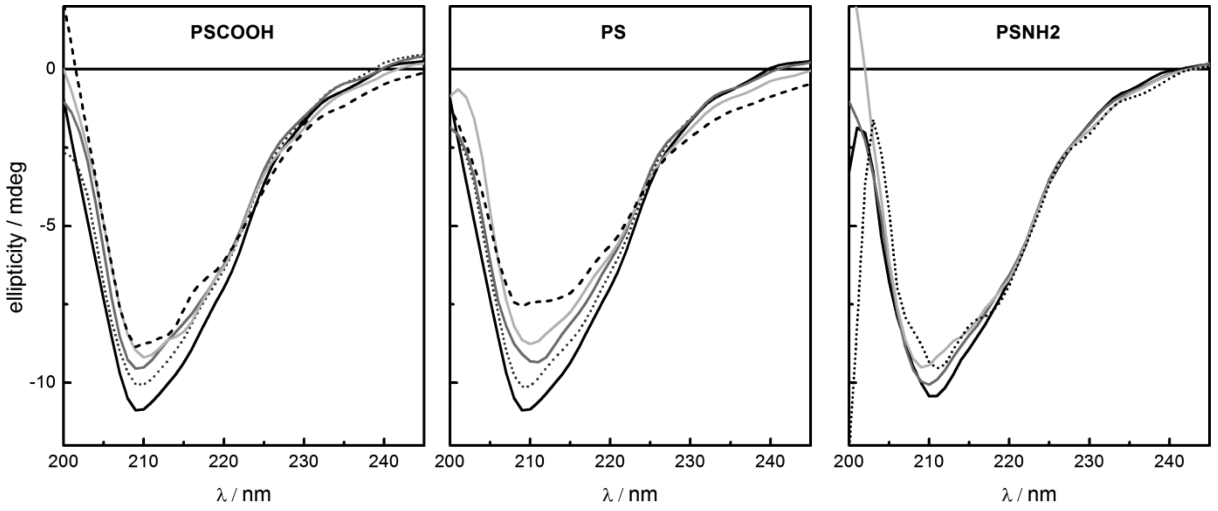

Figure 5. Far-UV CD spectra of HCAII in buffer (black) and with different nanoparticle concentrations: (dark gray, dotted) 0.005, (gray) 0.015, (light gray) 0.065, (black, dotted line) 0.1, and (black, dashed line) 0.115 mg/mL.

polystyrene nanoparticles in this study, suggesting stronger interactions with the enzyme.

The inhibition displayed by the negatively charged nanoparticles can have different explanations at the molecular level. First, the substrate, NPA, can be adsorbed or trapped at the nanoparticles' surface in a way that is inaccessible to the enzyme. Even though this effect is possible the substrate concentration is too high to be significantly decreased through binding in one layer on the nanoparticles. Second, the enzyme can be adsorbed on the nanoparticle surface in its native state in such a way that the accessibility to the active site is restricted which would lead to a decrease of the observed initial rate. Third, the enzyme can lose its tertiary structure due to the adsorption causing a loss in enzymatic efficiency. The latest hypotheses imply that only when adsorption take place the reaction is inhibited. In the case of polyelectrolyte coated gold nanoparticles, a fourth explanation is plausible. The sulfonate groups (on Au@PSS) and carboxylic groups (on Au@PAH@PAA) in the polyelectrolyte can be flexible enough to bind to the active site of the protein as free anions. Sulfonate and carboxylate anions together with wide range of other anions are known to inhibit HCAII to different extents.[30]

HCAII adsorbs at the negative nanoparticles surface as demonstrated by ITC and adsorption assay experiments. Considering the size of the enzyme, a prolate spheroid of 39 × 42 × 55 Å,[15] and the surface of the nanoparticles, a maximum amount of proteins on the particle surface and consequently the percentage of coverage can be calculated. In the case of PSCOOH, the coverage calculated from both experimental methods (Table 2) is close to 100% coverage, suggesting the formation of a monolayer of enzyme coating the nanoparticle. The formation of a monolayer is compatible with the results obtained from the DLS experiments when HCAII is titrated into a PSCOOH solution. The mean diameter of the PSCOOH nanoparticles increases progressively as the concentration of the protein increases (Figure 1). No significant broadening of the size distribution is observed, supporting that the increase in size is due to protein adsorption on the particle surface and not particle aggregation. The diameter progressively increases up to 12 nm. After that, addition of more protein does not result in further increase in size of the particles. This nanoparticle−protein complex of 56 nm is stable up to 24 h. A monolayer of native folded HCAII would increase the particle hydrodynamic diameter between 6 and 8 nm, lower than the observed increase, indicating the possibility of more than one layer of HCAII adsorbed in a native-like conformation. However, conformational changes of the protein upon adsorption could lead to a bigger contribution to the complex hydrodynamic diameter. In fact, it has been shown that the adsorption of HCAII on silica particles lead to conformational changes toward a more bulky molten-globule-like state.[29] The kinetic data also report coverage compatible with a monolayer of protein (Table 2). On the other hand, the protein coverage for PS according to the activity assay and the adsorption assay is less than one layer (Table 2). The coverage obtained by ITC is much lower, but this value is compromised by the aggregation of PS particles at high concentration when titrated with HCAII (Figure 1).

The equilibrium dissociation constants, K_d, obtained by the different techniques (Table 2) are in the lower micromolar region, indicating a low microscopic affinity (the affinity of each individual binding site). However, the large surface area of the particles has to be taken into account when comparing the total binding capacity of the nanoparticle. A single nanoparticle exposes to a protein a high amount of binding sites (400−500 in the cases presented in this work) that will result in macroscopic dissociation constants in the nanomolar region, i.e., high affinity.

The K_d values for the ITC and adsorption assay are of the same order of magnitude. However, K_{iapp} values obtained in the activity assays are 10-fold lower. K_{iapp} values depend differently on the substrate concentration and K_m according to the type of inhibition.[31] If the nanoparticle acts as a competitive inhibitior, it would block the access to the active site and compete with the substrate. In that case and under the experimental conditions chosen, the apparent inhibitor association constants should be equal to the inhibitor dissociation constant. However, the nanoparticle can also affect the conformation of the active site and therefore the affinity of the enzyme for the substrate as well as the rate constant of the enzymatic reaction. In that case, we would expect that $K_{iapp} \neq K_d$.[31] Other effects, such as interference of the substrate and the difference in protein concentration between ITC experiments and kinetic experiments, have been also suggested as causes for the

dx.doi.org/10.1021/la501413r | Langmuir 2014, 30, 9448−9456

difference in the binding constant values obtained with different techniques.[32,33] Overall, the data suggest that binding of the active site area to the nanoparticle surface and total blockage of the access to the active site are not the only explanations for the effects observed. Studies of the interaction of HCAII with silica particles show that the initial binding region of HCAII is not around the active site but in the regions around the N- and C-terminus of HCAII.[34,35] The initial binding causes some inactivation, but full inactivation is not observed until certain conformational changes in the active site region have taken place.[29]

Driving Forces of the Nanoparticle−HCAII Interaction. HCAII interacts and gets inhibited by negatively charged nanoparticles (both gold and polystyrene particles) but not positive ones, which suggests a role of electrostatic interactions in the adsorption process. The experimental pH is close to the pI of the enzyme (7.36),[36] rendering a slight negative charge on the protein. HCAII clearly interacts with the negatively charged nanoparticles used in this study, and the adsorption leads, in the case of negative charged polystyrene nanoparticles, to conformational changes as observed by CD spectroscopy. It is generally observed that proteins tend to adsorb more strongly to hydrophobic surfaces and to charged rather than uncharged ones.[2,14] Interactions with hydrophobic surfaces can be driven by the dehydration of the interface of the particle. Moreover, these surfaces promote changes in conformation on the protein to maximize also the interaction between protein and surface. In the case of hydrophilic surfaces the existence of attractive electrostatic interactions between protein and surface is required for the adsorption. The polystyrene nanoparticles are hydrophobic,[2] and therefore it is not surprising that HCAII interacts with those nanoparticles. Nevertheless, we see a different effect of the negative respect to the positively charged nanoparticles. While the PSCOOH and PS adsorb and inhibit HCAII, no effect is observed in the case of PSNH2 even though PSNH2 nanoparticles are also hydrophobic. Consequently, it can be concluded that hydrophobic interactions are not the only or the main driving forces in the adsorption process to polystyrene nanoparticles. Taking into account that the enzyme is slightly negative and that PSNH2 is positively charged, an initial electrostatic attraction at long distance would be expected between the HCAII and PSNH2. However, this interaction is not enough to form a stable PSNH2−HCAII complex. We should not forget that proteins are complex polymers with a distribution of negative and positive charges on the surface. Therefore, the net charge it is not always the main contributor to electrostatic attraction between protein and surfaces. Patches with certain local charge can drive the first binding event which can be followed by further rearrangements in conformation. In fact, adsorption of HCAII on negative silica nanoparticles was previously observed and explained based on the observation that the regions involved in the initial binding of HCAII to the silica particles are locally positive.[34,35] In a similar way, electrostatic attractions between positive patches on the protein surface and the negative nanoparticles can drive the initial adsorption of HCAII. However, no strong electrostatic attractions are created between PSNH2 and HCAII. Based on the CD data (Figure 5), it can be speculated that the PSNH2 surface does not promote the structural changes that the PSCOOH and PS surface does. Thus, the strong inner protein−particle surface interactions that may lead to a stable complex are not formed. Hence, the main forces involved in the initial binding events to polystyrene nanoparticles are electrostatic attractive forces between local patches at the protein surface and the particle.

Even if HCAII adsorbs at the particle surface of both PS and PSCOOH, the ITC data suggest that the driving forces in each case are different. For PSCOOH, ΔH of adsorption is positive. Taking into account that the adsorption process is spontaneous and therefore $\Delta G < 0$, entropic factors must be the main driving forces contributing to the enzyme adsorption. This is also supported by the positive entropic term obtained from the ITC data. In fact, the entropic factors have been highlighted as the main driving force in a number of cases regarding nanoparticle−protein interactions.[37,38] This entropic gain can be attributed to conformational changes in the protein that allow more structural freedom as well as release of counterions and hydration water from the contact area between nanoparticles and protein.[37,39,40] Therefore, the hydrophobic effect still has an important role as driving force for the interaction between HCAII and PSCOOH.

The interpretation of the enthalpic term is somewhat more challenging. Compensating contributions to the enthalpic factor can arise from specific and nonspecific electrostatic interactions and loss of favorable intramolecular interactions upon unfolding.[38] The results of it will give the sign of the enthalpic contribution. The adsorption on PS nanoparticles is exothermic ($\Delta H < 0$) with a negative entropic factor. This suggests that enthalpically favorable interactions are formed between the surface groups of the particle and the protein. Therefore, it is possible that upon adsorption initially driven by local electrostatic interactions positively charged residues can come into contact to the negatively charge surface to establish favorable interactions that will lead to a favorable enthalpy factor ($\Delta H < 0$). Similar exothermic peaks were also observed in the case of HSA binding to PSCOOH (Figure S6) as well as in the study of the adsorption of BSA to polystyrene particle of different surface coating.[41]

In order to establish strong protein−nanoparticle interactions, the protein may change its conformation at the particle surface. It has been reported that HCAII in the presence of silica nanoparticles adsorb initially in a native-like state and change conformation after prolonged incubation.[17,29,42] The addition of PS and PSCOOH nanoparticles clearly affects the secondary structure of HCAII. Figure 5 shows that the CD signal decreases with the nanoparticle concentrations, indicating a loss of secondary structure. However, in the same manner as the inactivation, the conformational changes are observed earlier than in the case of silica particles (minutes instead of days).[29,35] The more severe conformational changes observed for HCAII in the presence of PS nanoparticles would allow establishing favorable interactions with the nanoparticle surface and explain the enthalpic contribution to the adsorption process. Stronger nanoparticle−protein interactions will lead to favorable enthalpy values in addition to restricting the mobility of the protein (decrease of entropy) compensating for the entropically favorable surface dehydration and counterion release. The balance of the entropic and enthalpic contributions results in a favorable interaction between between HCAII and PS.

■ CONCLUSIONS

The enzymatic activity of HCAII is affected by negatively charged nanoparticles. Negatively charged polystyrene nanoparticles inhibit HCAII fast and efficiently. The inhibition requires the adsorption of the enzyme on the particle surface

dx.doi.org/10.1021/la501413r | Langmuir 2014, 30, 9448−9456

and subsequent conformational changes. Nevertheless, the driving forces for the adsorption of HCAII on PSCOOH and PS nanoparticle differ. Even though hydrophobic interactions have been suggested to be an important contributor to protein adsorption, our data indicate that local electrostatic interactions drive the first binding events. This is supported by the fact that positively charged hydrophobic PSNH2 nanoparticles do not adsorb and inhibit the enzyme. However, the particular chemistry of the nanoparticle surface also plays a role in the final inhibitory effect. The stoichiometry of the complex and the microscopic dissociation constant varies depending on the particular surface modification of the nanoparticle. Adsorption to PSCOOH is entropically driven while adsorption to PS is enthalpically driven even though both particles have the same charge. To conclude, in order to develop a working enzyme−nanoparticle device, a detailed analysis of the enzyme−nanoparticle interactions would be advised. For each enzyme−nanoparticle case, a different combination of driving forces applies, and therefore the behavior of the enzyme in a bionanodevice cannot be easily predicted.

■ ASSOCIATED CONTENT

Supporting Information

Details for ITC data analysis and figures for the variation of particle diameter at low particle concentration, ITC data for human albumin−PSCOOH adsorption, and adsorption assay for PSNH2. This material is available free of charge via the Internet at http://pubs.acs.org.

■ AUTHOR INFORMATION

Corresponding Author

*E-mail Celia.Cabaleiro-Lago@biochemistry.lu.se (C.C.-L.).

Author Contributions

The manuscript was written through contributions of all authors. All authors have given approval to the final version of the manuscript. A.A. and C.C.L. designed, performed, and analyzed the experiments. IPS helped to design the experiments.

Notes

The authors declare no competing financial interest.

■ ACKNOWLEDGMENTS

This study was funded by the Swedish Research Council (VR), the Crafoord Foundation, and the Royal Physiographic Society. The authors acknowledge financial support from the European Commission under the Seventh Framework Program by means of the grant agreement for the Integrated Infrastructure Initiative N. 262348 European Soft Matter Infrastructure (ESMI). We thank Cristina Fernández-López for her help regarding the synthesis of gold nanoparticles.

■ REFERENCES

(1) Rabe, M.; Verdes, D.; Seeger, S. Understanding protein adsorption phenomena at solid surfaces. *Adv. Colloid Interface Sci.* **2011**, *162* (1-2), 87−106.

(2) Haynes, C. A.; Norde, W. Globular proteins at solid/liquid interfaces. *Colloids Surf., B* **1994**, *2* (6), 517−566.

(3) Yonzon, C. R.; Stuart, D. A.; Zhang, X. Y.; McFarland, A. D.; Haynes, C. L.; Van Duyne, R. P. Towards advanced chemical and biological nanosensors - an overview. *Talanta* **2005**, *67* (3), 438−448.

(4) Rosi, N. L.; Mirkin, C. A. Nanostructures in biodiagnostics. *Chem. Rev.* **2005**, *105* (4), 1547−1562.

(5) Caruso, F.; Schuler, C. Enzyme multilayers on colloid particles: Assembly, stability, and enzymatic activity. *Langmuir* **2000**, *16* (24), 9595−9603.

(6) Vinoba, M.; Bhagiyalakshmi, M.; Jeong, S. K.; Nam, S. C.; Yoon, Y. Carbonic anhydrase immobilized on encapsulated magnetic nanoparticles for CO_2 sequestration. *Chem.—Eur. J.* **2012**, *18* (38), 12028−12034.

(7) Zhang, S.; Wright, G.; Yang, Y. Materials and techniques for electrochemical biosensor design and construction. *Biosens. Bioelectron.* **2000**, *15* (5-6), 273−282.

(8) Banerjee, I.; Pangule, R. C.; Kane, R. S. Antifouling coatings: Recent developments in the design of surfaces that prevent fouling by proteins, bacteria, and marine organisms. *Adv. Mater.* **2011**, *23* (6), 690−718.

(9) You, C.-C.; De, M.; Han, G.; Rotello, V. M. Tunable inhibition and denaturation of α-chymotrypsin with amino acid-functionalized gold nanoparticles. *J. Am. Chem. Soc.* **2005**, *127* (37), 12873−12881.

(10) Maccormack, T. J.; Clark, R. J.; Dang, M. K. M.; Ma, G.; Kelly, J. A.; Veinot, J. G. C.; Goss, G. G. Inhibition of enzyme activity by nanomaterials: Potential mechanisms and implications for nanotoxicity testing. *Nanotoxicology* **2012**, *6* (5), 514−525.

(11) Innocenti, A.; Durdagi, S.; Doostdar, N.; Strom, T. A.; Barron, A. R.; Supuran, C. T. Nanoscale enzyme inhibitors: Fullerenes inhibit carbonic anhydrase by occluding the active site entrance. *Biorg. Med. Chem.* **2010**, *18* (8), 2822−2828.

(12) Saada, M.-C.; Montero, J.-L.; Vullo, D.; Scozzafava, A.; Winum, J.-Y.; Supuran, C. T. Carbonic anhydrase activators: Gold nanoparticles coated with derivatized histamine, histidine, and carnosine show enhanced activatory effects on several mammalian isoforms. *J. Med. Chem.* **2011**, *54* (5), 1170−1177.

(13) Stiti, M.; Cecchi, A.; Rami, M.; Abdaoui, M.; Barragan-Montero, V.; Scozzafava, A.; Guari, Y.; Winum, J.-Y.; Supuran, C. T. Carbonic anhydrase inhibitor coated gold nanoparticles selectively inhibit the tumor-associated isoform IX over the cytosolic isozymes I and II. *J. Am. Chem. Soc.* **2008**, *130* (48), 16130.

(14) Norde, W. Driving forces for protein adsorption at solid surfaces. *Macromol. Symp.* **1996**, *103*, 5−18.

(15) Krishnamurthy, V. M.; Kaufman, G. K.; Urbach, A. R.; Gitlin, I.; Gudiksen, K. L.; Weibel, D. B.; Whitesides, G. M. Carbonic anhydrase as a model for biophysical and physical-organic studies of proteins and protein-ligand binding. *Chem. Rev.* **2008**, *108* (3), 946−1051.

(16) Whitney, P. L.; Nyman, P. O.; Malmstro, Bg. Inhibition and chemical modifications of human erythrocyte carbonic anhydrase B. *J. Biol. Chem.* **1967**, *242* (18), 4212.

(17) Billsten, P.; Freskgard, P. O.; Carlsson, U.; Jonsson, B. H.; Elwing, H. Adsorption to silica nanoparticles of human carbonic anhydrase ii and truncated forms induce a molten-globule-like structure. *FEBS Lett.* **1997**, *402* (1), 67−72.

(18) Vinoba, M.; Lim, K. S.; Lee, S. H.; Jeong, S. K.; Alagar, M. Immobilization of human carbonic anhydrase on gold nanoparticles assembled onto amine/thiol-functionalized mesoporous SBA-15 for biomimetic sequestration of CO_2. *Langmuir* **2011**, *27* (10), 6227−6234.

(19) Shin, H. J.; Hwang, I. W.; Hwang, Y. N.; Kim, D.; Han, S. H.; Lee, J. S.; Cho, G. J. Comparative investigation of energy relaxation dynamics of gold nanoparticles and gold-polypyrrole encapsulated nanoparticles. *J. Phys. Chem. B* **2003**, *107* (20), 4699−4704.

(20) Turkevich, J.; Stevenson, P. C.; Hillier, J. A study of the nucleation and growth processes in the synthesis of colloidal gold. *Discuss. Faraday Soc.* **1951**, No. 11, 55.

(21) Schneider, G.; Decher, G. Functional core/shell nanoparticles via layer-by-layer assembly. Investigation of the experimental parameters for controlling particle aggregation and for enhancing dispersion stability. *Langmuir* **2008**, *24* (5), 1778−1789.

(22) Rodriguez-Fernandez, J.; Perez-Juste, J.; Javier Garcia de Abajo, F.; Liz-Marzan, L. M. Seeded growth of submicron Au colloids with quadrupole plasmon resonance modes. *Langmuir* **2006**, *22* (16), 7007−7010.

(23) Pastoriza-Santos, I.; Perez-Juste, J.; Liz-Marzan, L. M. Silica-coating and hydrophobation of CTAB-stabilized gold nanorods. *Chem. Mater.* **2006**, *18* (10), 2465−2467.
(24) Morrison, J. F. Kinetics of reversible inhibtion of enzyme-catalysed reactions by tight-binding inhibitors. *Biochim. Biophys. Acta* **1969**, *185* (2), 269.
(25) Liz-Marzán, L. M. Tailoring surface plasmons through the morphology and assembly of metal nanoparticles. *Langmuir* **2006**, *22* (1), 32−41.
(26) Freskgard, P. O.; Martensson, L. G.; Jonasson, P.; Jonsson, B. H.; Carlsson, U. Assigment of the contribution of the tryptophan residues to the circular-dichroism spectrum of human carbonic anhydrase 2. *Biochemistry* **1994**, *33* (47), 14281−14288.
(27) Pasquato, L.; Pengo, P.; Scrimin, P. Functional gold nanoparticles for recognition and catalysis. *J. Mater. Chem.* **2004**, *14* (24), 3481−3487.
(28) Katz, E.; Willner, I. Integrated nanoparticle-biomolecule hybrid systems: Synthesis, properties, and applications. *Angew. Chem., Int. Ed.* **2004**, *43* (45), 6042−6108.
(29) Karlsson, M.; Martensson, L. G.; Jonsson, B. H.; Carlsson, U. Adsorption of human carbonic anhydrase II variants to silica nanoparticles occur stepwise: Binding is followed by successive conformational changes to a molten-globule-like state. *Langmuir* **2000**, *16* (22), 8470−8479.
(30) De Simone, G.; Supuran, C. T. (In)organic anions as carbonic anhydrase inhibitors. *J. Inorg. Biochem.* **2012**, *111*, 117−129.
(31) Copeland, R. A. *Enzymes: A Practical Introduction to Structure, Mechanism, and Data Analysis*; VCH Publishers: New York, 1996; p 306.
(32) De, M.; You, C.-C.; Srivastava, S.; Rotello, V. M. Biomimetic interactions of proteins with functionalized nanoparticles: A thermodynamic study. *J. Am. Chem. Soc.* **2007**, *129* (35), 10747−10753.
(33) Linse, S.; Jonsson, B.; Chazin, W. J. The effect of protein-concentration on ion-binding. *Proc. Natl. Acad. Sci. U. S. A.* **1995**, *92* (11), 4748−4752.
(34) Karlsson, M.; Carlsson, U. Protein adsorption orientation in the light of fluorescent probes: Mapping of the interaction between site-directly labeled human carbonic anhydrase ii and silica nanoparticles. *Biophys. J.* **2005**, *88* (5), 3536−3544.
(35) Lundqvist, M.; Andresen, C.; Christensson, S.; Johansson, S.; Karlsson, M.; Broo, K.; Jonsson, B. H. Proteolytic cleavage reveals interaction patterns between silica nanoparticles and two variants of human carbonic anhydrase. *Langmuir* **2005**, *21* (25), 11903−11906.
(36) Funakoshi, S.; Deutsch, H.F. Human carbonic anhydrases. II. Some physicochemical properties of native isozymes and of similar isozymes generated in vitro. *J. Biol. Chem.* **1969**, *244* (13), 3438−3446.
(37) Norde, W.; Lyklema, J. Adsoprtion of human-plasma albumin and bovine pancreas ribonuclease at negatively charged polystyrene surfaces. 5. Micro-calorimetry. *J. Colloid Interface Sci.* **1978**, *66* (2), 295−302.
(38) Haynes, C. A.; Norde, W. Structure and stabilities of adsorbed proteins. *J. Colloid Interface Sci.* **1995**, *169* (2), 313−328.
(39) Roth, C. M.; Sader, J. E.; Lenhoff, A. M. Electrostatic contribution to the energy and entropy of protein adsorption. *J. Colloid Interface Sci.* **1998**, *203* (1), 218−221.
(40) Geng, X. P.; Zheng, M. R.; Wang, B. H.; Lei, Z. M.; Geng, X. D. Fractions of thermodynamic functions for native lysozyme adsorption onto moderately hydrophobic surface. *J. Therm. Anal. Calorim.* **2008**, *93* (2), 503−508.
(41) Baier, G.; Costa, C.; Zeller, A.; Baumann, D.; Sayer, C.; Araujo, P. H. H.; Mailaender, V.; Musyanovych, A.; Landfester, K. Bsa adsorption on differently charged polystyrene nanoparticles using isothermal titration calorimetry and the influence on cellular uptake. *Macromol. Biosci.* **2011**, *11* (5), 628−638.
(42) Lundqvist, M.; Sethson, I.; Jonsson, B. H. High-resolution 2D H-1-N-15 NMR characterization of persistent structural alterations of proteins induced by interactions with silica nanoparticles. *Langmuir* **2005**, *21* (13), 5974−5979.